EFFICIENCY OF DEFORMABLE AND SEGMENTED MIRRORS IN CORRECTION OF TURBULENCE–INDUCED DISTORTIONS OF A BEAM WAVE FRONT

F.Yu. Kanev, V.P. Lukin, and B.V. Fortes

Institute of Atmospheric Optics,
Siberian Branch of the Russian Academy of Sciences, Tomsk
Received September 29, 1992

The point spread function (PSF) for a ground–based telescope is calculated for two types of wave–front correctors, i.e., deformable and segmented mirrors. The deformable mirror is assumed to be a thin square plate fixed at its center and deformed with a system of lateral forces applied to 20 points. The segmented corrector is a set of square segments with three degrees of freedom, the number of elements varies from 1 to 16. The wave–front distortions are of the Kolmogorov spectrum and are considered to be known for each random realization. It is shown that the PSF calculated for a 9–element segmented corrector (27 degrees of freedom) is close to that obtained for the deformable mirror with 27 degrees of freedom.

INTRODUCTION

The problem of compensation for atmospheric distortions of a beam wave front has been studied sufficiently long. The first papers on this subject were published in the mid–1960s, Ref. 1. At that time, however, the engineering base gaves no way for designing the efficient devices for compensating for atmospheric distortions. In recent years much progress has been reached in developing wave–front distortion meters and correctors and then fitting the optical facilities operating under atmospheric distortions with these devices.[2–5] In this connection an increased interest of researchers is observed to the theoretical works concerning with selection of an optical design and configuration of the wave–front corrections.[6–9]

There are two major classes of wave–front correctors such as deformable and segmented mirrors. The efficiency of a segmented mirror with segments of hexagonal shape was considered in Ref. 11. As shown in this paper, for the resolution of the ground–based telescope to be close to a diffraction limit such a segment needs to be only three Fried's radii in size.[6] Described in Ref. 10 is a flexible corrector with different functions of response as well as the formula for estimating variance of residual wave–front distortions. However, the system's PSF was not found, and the functions of response were not determined for a real flexible plate. In Ref. 12, the mirror–response functions were calculated while the residual wave–front distortions were not calculated.

Thus the available literature does not contain the data which could provide for a direct comparison between the efficiencies of flexible and segmented wave–front correctors for compensating for turbulence–induced distortions of an image. Such a comparison has previously been done in the problem of compensation for distortions occurring at thermal blooming of a high–power beam along a vertical path.[11] We used a model of a segmented mirror with hexagonal elements and compared its efficiency with that of a low–order aberration correction, i.e., approximated a deformable mirror with a modal corrector. This paper concerns the segmented corrector with squared elements and the model of a flexible square plate which is deformed with 20 servodrives used as a deformable mirror. The resultant PSF of the two systems was compared in the course of varying a number of elements of the segmented corrector.

2. MODEL OF AN OPTICAL SYSTEM

In our study we have considered a telescope with a square entrance pupil of the cross–size $D = 1$ m. The point spread function was calculated using one of the following methods.

The first method conventionally employed for calculating the PSF consists in determining the discrete Fourier transform (DFT) of a two–dimensional set of complex numbers $U(l, m)$, $l, m = 1, \dots N$ (N is the size of the set) representing discrete (with a spatial step $\Delta x = \Delta y$) distribution of the optical wave complex amplitude $U(x, y)$ in the plane of the telescope aperture. The second method traditionally used for calculating propagation of paraxial beams involves three stages: (1) computation of the DFT of the field complex amplitude, (2) multiplying the field spatial spectrum by a filtering function related to propagation to a distance f, Ref. 13, and (3) calculation of the inverse DFT whose result is the distribution of the field complex amplitude in the plane $z = f$. First, in the plane $z = 0$, the complex amplitude $U(x, y)$ is multiplied by a complex factor

$$C(x, y) = \exp\left\{\frac{ik}{2f}(x^2 + y^2)\right\} \quad (1)$$

corresponding to the field focusing on the plane $z = f$. Here $k = 2\pi/\lambda$ is the wave number and λ is the radiation wavelength.

The first method was primarily used in calculating the PSF without a correction. The second method is convenient because of the possibility of varying the scale of intensity distribution in the focal plane by changing the focal length f. When

$$f = f_1 = (\Delta x)^2\, N/\lambda \quad (2)$$

the intensity distribution $I(l, m)$ over the focal plane calculated by the method of spatial frequency filtration

0235-6880/92/12 852-03 $02.00

(SFF) is practically identical to that calculated by the DFT method. When the focal length is 2 f_1 the intensity distribution becomes twice as wide, when $f = f_1/2$ it is twice as narrow, and so on. In this case only the linear scale changes and the angular intensity distribution is kept constant. The SFF method is convenient when calculating the corrected PSF whose width approaches the diffraction limit, and it has therefore become necessary to increase the number of points of a calculational grid which fall within the effective size of a focal spot.

The effect of turbulent fluctuations of the refractive index of the atmosphere was taken into account in approximation of a phase screen positioned in the plane of the telescope aperture and distorting only the wave–front shape of the initially plane wave. The spectral density of phase fluctuations was taken in the form

$$F_s(\mathrm{k}) = 0.489\, r_0^{-5/3}(\mathrm{k}^2 + \mathrm{k}_0^2)^{-11/6}\ , \tag{3}$$

where

$$r_0 = \Big(k^2 \int C_n^2(h)\,\mathrm{d}h\Big)^{-5/6} \tag{4}$$

is the Fried's coherence radius, $\kappa_0 = 2\pi/L_0$, and L_0 is the outer scale of turbulence. Different estimates of outer scale of the turbulence exist: from tens and hundreds of meters to tens kilometers. In our calculations L_0 =1000 m.

Spatial scales of phase fluctuations satisfying the condition $2\pi/\kappa < N\Delta x = G$, where N is the dimensionality of the calculational grid along the X and Y axes were generated by calculating the DFT of a set of read–outs of random spectral–amplitude realizations $A_s(\kappa_{x\,l}\,,\ \kappa_{y\,m})$ satisfying the condition

$$<A_s(\kappa_{x\,l}\,,\ \kappa_{y\,m})\,|^2> = F_s(\kappa_{x\,l}\,,\ \kappa_{z\,m})\ , \tag{5}$$

where the angular brackets indicate averaging over a statistical ensemble. To take into account the spatial scales larger than the dimensionality of the calculational grid G we added aberrations calculated as a sum of the first 28 Zernike polynomials[7,8] and the coefficients produced with a random–number generator as independent random values distributed following the normal distribution law with zero mean and the variance

$$\sigma_n^2 = 8\pi(n + 1) \int\limits_0^{2\pi/G} \mathrm{k}\mathrm{d}\mathrm{k} F_s(\mathrm{k})\, \frac{J_n^2(\mathrm{k}R)}{(\mathrm{k}R)^2}\ , \tag{6}$$

where n is the radial power of the corresponding polynomial.

3. MODELS OF MIRRORS

Action of the segmented corrector was simulated as subtraction of a constant component and linear components calculated by the method of least squares, for the rms error of residual distortions to be minimum, from the distorted wave– front within each element of the corrector.

The statistical deflection $W(x, y)$ of a flexible mirror was described by the equation of the biharmonic type[14]

$$D\left(\frac{\partial^4 W}{\partial x^4} + 2\,\frac{\partial^4 W}{\partial x^2 \partial y^2} + \frac{\partial^4 W}{\partial y^4}\right) = g\,(x,\ y)\ , \tag{7}$$

where $g\,(x,\ y)$ is the transverse load and D is the cylindrical rigidity. For the used mirror with unfastened edges the conditions at the contour were given as

$$D\,\left(\frac{\partial^2 W}{\partial n^2} + \sigma\,\frac{\partial^2 W}{\partial \tau^2}\right)\Bigg|_{L_j} = 0, \tag{8}$$

where $\partial/\partial n$ and $\partial/\partial\tau$ are the derivatives with respect to the normal and tangent to the surface, respectively, and σ is the Poisson coefficient. The condition at the central hinged point is

$$W = 0,\ D\left(\frac{\partial^2 W}{\partial n^2} + \sigma\,\frac{\partial^2 W}{\partial \tau^2}\right) = 0\ . \tag{9}$$

4. THE RESULTS OF MODELING

The PSF determination was determined for the visible spectral range at the wavelength $\lambda = 0.55$ μm. The coherence radius r_0 was assumed to have two values: 20 cm (Fig. 1*a*) and 10 cm (Fig. 1*b*) ($D/r_0 = 5$ and 10, respectively). The calculations were made for a segmented corrector whose number of elements varied between 1 (3 degrees of freedom) and 16 (48 degrees of freedom) and for a deformable corrector (20 degrees of freedom). In each of the figures, the angular distance α in seconds of arc is plotted on the OX axis, and the radial cross section of the PSF normalized to diffraction maximum is plotted on the OY axis. The PSF was averaged over random realizations of the wave–front distortions whose numbers were 100–300 for system without a correction and 10–30 with correction of the wave–front distortions. Supplementary results are listed in Tables I and II. These are the values of the ratio of the Strehl's number St to the total width of the PSF at half maximum (FWHM) as a function of the number of degrees of freedom of the corrector N_c. The last lines of the tables are related to the deformable mirror, and the first lines are the uncorrected PSF.

As follows from the results, the efficiency of compensation for distortions with a segmented mirror increases proportionally to the number of its elements (the number of coordinates under control). In this case approximately the same results were obtained for a segmented mirror with 27 degrees of freedom and for a deformable mirror with 20 degrees of freedom. The efficiency of the mirror is likely to be mostly determined by the number of coordinates under control and virtually does not change when passing from a segmented mirror to a deformable one.

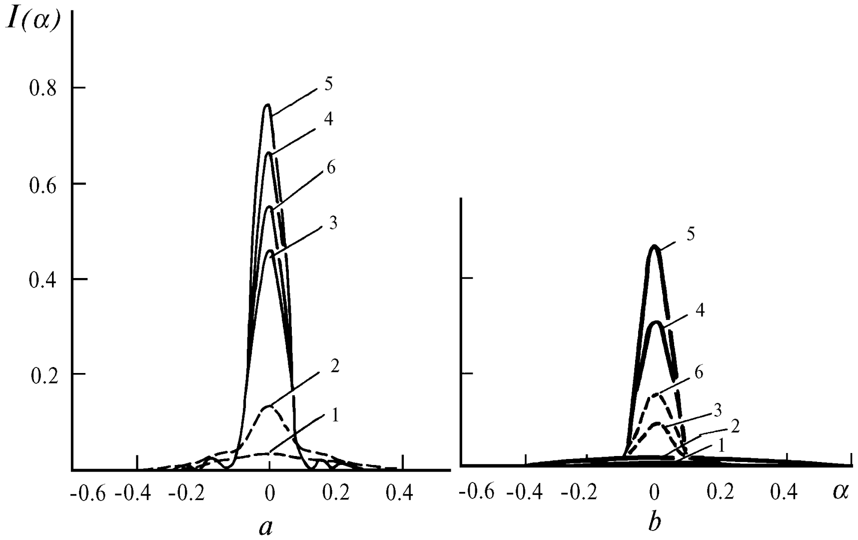

FIG. 1. PSF of an adaptive telescope vs a number of degrees of freedom of an active element:1) without correction, 2) three degrees of freedom (a segmented mirror and 1 element), 3) 12 degrees of freedom (a segmented mirror and 4 elements), 4) 27 degrees of freedom (a segmented mirror and 9 elements), 5) 48 degrees of freedom (a segmented mirror and 16 elements), 6) 20 degree of freedom (a deformable corrector and 20 servodrives).
a) r_0 = 20 cm and *b)* r_0 = 10 cm.

TABLE I.

N_c	St	FWHM
0	0.03	0.50″
3	0.14	0.14″
12	0.45	0.10″
27	0.67	0.10″
48	0.75	0.10″
20	0.55	0.10″

TABLE II.

N_c	St	FWHM
0	0.008	1.1″
3	0.017	0.64″
12	0.09	0.11″
27	0.31	0.10″
48	0.46	0.10″
20	0.15	0.11″

REFERENCES

1. D.L. Fried, J. Opt. Soc. Am. **56**, No. 10, 1372–1379 (1966).
2. F. Merkle, Tech. Rept. LEST Foundat., No. **28**, 35–54 (1987).
3. F. Dickman, Nature **341**, No. 26, 675 (1989).
4. R.N. Wilson, F. Franza, and L. Noethe, J. Modern Optics **34**, No. 4, 485–509 (1987).
5. R.R. Dunn, Techn. Rept. LEST Foundat. **28**, 87–106 (1987).
6. D.L. Fried, Proc. IEEE **55**, 57–67 (1967).
7. R.J. Noll, J. Opt. Soc. Am. **66**, No. 3, 207–211 (1976).
8. N. Roddier, Opt. Eng. **29**, No. 10, 1174–1180 (1990).
9. R. Buckley, J. Atmos. Terr. Phys. **37**, 1431–1446 (1975).
10. R.K. Tyson, Opt. Eng. **29**, No. 10, 1165–1173 (1990).
11. P.A. Konyaev, V.P. Lukin, and B.V. Fortes, Atm. Opt. **3**, No. 12, 1157–1162 (1990).
12. P.K. Mehta, Opt. Engineering **29**, No. 10, 1213–1222 (1990).
13. J.W. Goodman, *Introduction into Fourier Optics* (McGraw Hill, New Jork, 1968).
14. P.M. Ogibalov, *Deflection, Stability, and Vibrations of Plates,* (Izd. Moscow State University, Moscow 1958).